JOURNAL OF Materials CHEMISTRY

Variable temperature structural study of bismuth lead vanadate, $BiPb_2VO_6$

Ivana Radosavljevic Evans,* John S. O. Evans and Judith A. K. Howard

Department of Chemistry, University of Durham, Science Site, South Road, Durham, England, UK DH1 3LE. E-mail: Ivana.Radosavljevic@durham.ac.uk

Received 18th March 2002, Accepted 7th June 2002
First published as an Advance Article on the web 23rd July 2002

At room temperature, monoclinic $BiPb_2VO_6$ is a polar, noncentrosymmetric, second harmonic generation active material and its crystal structure is among the more complex to be solved *ab initio* from powder diffraction data. In its stability range, $BiPb_2VO_6$ also exists in a high symmetry, orthorhombic form. Both phases have been structurally characterized by a combination of X-ray and neutron diffraction data. Their mutual relationship, as well as that to the known compounds of the BiM_2AO_6 (M = Mg, Ca, Mn, Cu, Zn, Pb and A = P, V, As) family, has been established.

Introduction

Bi(III)-containing oxides have been extensively studied owing to their interesting and potentially applicable physical properties, including ferroelectricity,[1] ionic conductivity[2] and catalytic activity.[3] In particular, bismuth vanadates and their derivatives have been found to exhibit many of these properties, which has been attributed to the presence of structural features such as lone pair species and tetrahedral groups[4] or highly polarizable cation networks and readily mobile oxide ions.[5]

A number of ternary oxides with the general formula BiM_2AO_6 (M = Mg, Ca, Mn, Cu, Zn, Pb and A = V, As, P) have been reported.[6–17] They have been described as consisting of $(BiO_2)^-$ chains, isolated AO_4^{3-} tetrahedra and interspersed M cations. Differences between crystal structures of individual members of this family have been attributed to variations in the mutual orientation of these building units and in some cases these variations result in the presence of a specific physical property in the compound. For example, $BiCa_2VO_6$, $BiCa_2AsO_6$ and $BiCd_2VO_6$ are polar and second harmonic generation active owing to the AO_4 tetrahedra in these phases all pointing in the same direction (the polar axis of the crystal).

$BiPb_2VO_6$ was first reported in 1995 and described as apparently unrelated to the other BiM_2AO_6 phases.[14] We have since solved its crystal structure using a novel approach of simulated annealing applied simultaneously to X-ray and neutron diffraction data.[17] $BiPb_2VO_6$ undergoes a series of phase transitions between room temperature and its melting point at 780 °C.[15] This is an interesting system, since it involves two stable phases (α-$BiPb_2VO_6$ at room temperature and δ-$BiPb_2VO_6$ above 630 °C). However, depending on the kinetics of heating, a metastable β-$BiPb_2VO_6$ may form at 415 °C, which either converts directly into δ-$BiPb_2VO_6$ at 475 °C or undergoes decomposition followed by the formation of δ-$BiPb_2VO_6$ at 630 °C. The cooling process is always accompanied by a direct phase change from δ-$BiPb_2VO_6$ to α-$BiPb_2VO_6$ at about 450 °C. At room temperature, α-$BiPb_2VO_6$ is second harmonic generation active.[17]

In this paper we report the crystal structure of δ-$BiPb_2VO_6$ and describe its structural relationship to α-$BiPb_2VO_6$ and other phases of the BiM_2AO_6 family.

Experimental

Polycrystalline $BiPb_2VO_6$ samples were prepared by solid state reactions of stoichiometric quantities of Bi_2O_3, PbO and NH_4VO_3 at 720 °C. Synchrotron X-ray diffraction data for structure solution of α-$BiPb_2VO_6$ were collected in the capillary mode at beam line X7A of the Brookhaven NSLS, using a wavelength of 0.57775 Å. All variable temperature powder X-ray diffraction data were collected using a Bruker AXS D8 Advance diffractometer equipped with an Anton Paar HTK1200 high temperature stage and a Braun linear PSD. Data were collected in the 2θ range between 10 and 120° in 0.014° steps, using a counting time of 0.5 s step^{-1}.

Time-of-flight neutron diffraction data were collected on the High Resolution Powder Diffractometer (HRPD) at the ISIS neutron facility, Rutherford Appleton Labs, UK. Approximately 8 g of sample were loaded into a standard vanadium sample can and placed into a Rutherford Furnace. Data were collected at room temperature for approximately 25 μA h (~5 hours) using a time of flight range of 30–130 ms (d = 0.6–2.7 Å). The same range was used for a data collection at 680 °C, but the collection time was approximately 9 hours.

Results and discussion

Structure of α-$BiPb_2VO_6$

We have recently solved the structure of α-$BiPb_2VO_6$ using a combination of direct methods[18] and simulated annealing[19] applied simultaneously to synchrotron X-ray and constant wavelength neutron powder diffraction data.[17] It crystallizes in space group *Pn*, with cell parameters of a = 7.71538(1) Å, b = 5.84871(1) Å, c = 29.08237(3) Å and β = 94.25489(4)°. Initial refinements were performed using a relatively low resolution neutron data set. We have now refined this model using a time-of-flight neutron diffraction data set of significantly higher resolution. A total of 96 structural parameters were refined: 4 cell parameters for neutron data; 4 cell parameters for synchrotron data; 36 positional parameters and 1 isotropic temperature factor for Bi/Pb atoms; 3 rotations and 3 translations for each of the four unique rigid VO_4 groups and 1 isotropic temperature factor for rigid VO_4 groups; the average V–O bond length; 24 positional parameters and 1 isotropic temperature factor for tetrahedrally coordinated oxygen atoms. This led to final agreement factors of: overall wR_p = 4.062%, wR_p = 4.511% and R_{Bragg} = 2.275% for X-ray data and wR_p = 3.804% and R_{Bragg} = 1.941% for neutron data. The final Rietveld plots obtained for the structure are shown in Fig. 1. The atomic coordinates obtained are given in Table 1.

Views of the unit cell of α-$BiPb_2VO_6$ are given in Fig. 2. The

 DOI: 10.1039/b202648a

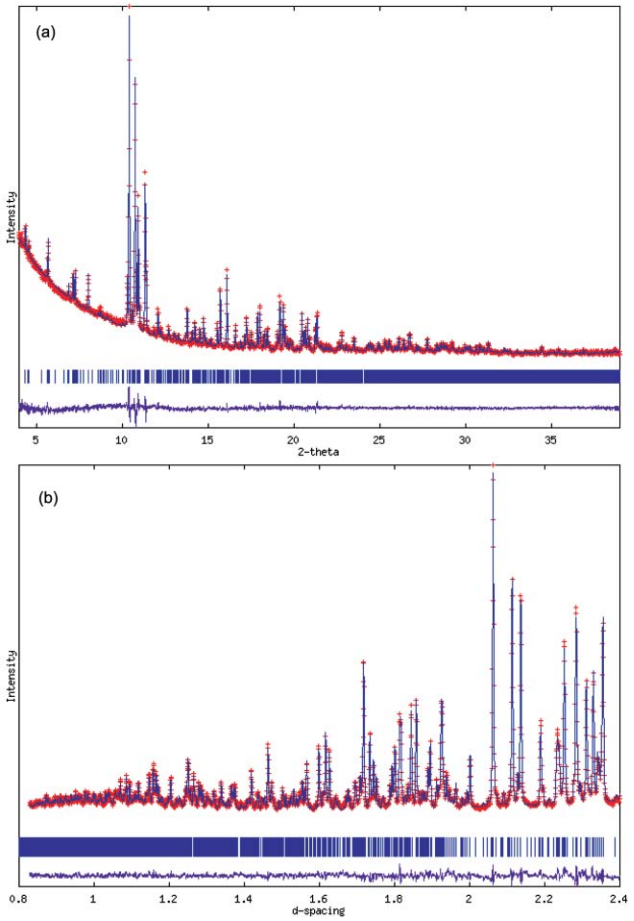

Fig. 1 Final Rietveld plots for (a) X-ray and (b) time-of-flight neutron data for α-$BiPb_2VO_6$.

crystal structure can be described as consisting of infinite chains of edge-sharing OBi_2Pb_2 tetrahedra running along the crystallographic *b* axis, with interspersed isolated VO_4 tetrahedral groups. The average V–O bond length is 1.7099(2) Å. Typical Bi/Pb environments are geometrically irregular and consist of up to five oxygen atoms at distances between 2.2 and 2.6 Å, with the coordination sphere completed by two to three oxygens up to 3 Å away. Eight crystallographically unique oxygen atoms are tetrahedrally coordinated by Bi/Pb, with bond lengths ranging from 2.2 to 2.6 Å. They form OBi_2Pb_2 tetrahedral units that share edges in a pattern similar to that found in the fluorite structure type.

Structure of δ-$BiPb_2VO_6$

Above 630 °C $BiPb_2VO_6$ adopts the so-called δ phase. Its unit cell has been reported as tetragonal with $a = 12.110(2)$ Å and $c = 9.472(8)$ Å.[14] The relationship between this unit cell and that of α-$BiPb_2VO_6$ was determined from three low angle reflections in the two patterns. The corresponding transformation matrix was then applied to the coordinates of Bi, Pb and V atoms obtained for α-$BiPb_2VO_6$ and the symmetry was reduced to *P*1. This preliminary model was then refined and it gave an excellent fit to the observed high temperature X-ray data, but the question of the true space group of δ-$BiPb_2VO_6$ remained to be addressed.

Although a model independent Pawley fit[20] performed using a tetragonal unit cell in space group $I4_1/amd$ was successful, attempts to obtain a satisfactory fit using a structural model in this space group failed. A close inspection of the metal positions in space group *P*1 revealed that the atomic arrangement in the structure was more likely to adopt the C-centered orthorhombic space group *Cmcm*.

Table 1 Atomic coordinates for α-$BiPb_2VO_6$[a]

Site	*x*	*y*	*z*	U_{iso}/Å^2
Bi1	0.0742(1)	0.4977(2)	0.20105(4)	0.02730(3)
Bi2	0.8130(2)	−0.0123(2)	0.15765(4)	0.02730(3)
Bi3	0.61952(8)	0.0058(2)	0.89678(2)	0.02730(3)
Bi4	0.3953(2)	0.4952(2)	0.44712(5)	0.02730(3)
Pb1	0.5941(2)	0.0362(2)	0.37640(4)	0.02730(3)
Pb2	0.8209(2)	0.4772(2)	0.82421(4)	0.02730(3)
Pb3	0.8833(2)	0.0259(2)	0.28210(4)	0.02730(3)
Pb4	0.1227 (2)	0.4814(2)	0.72971(4)	0.02730(3)
Pb5	0.2066(1)	−0.0195(2)	0.52336(4)	0.02730(3)
Pb6	1.0322(1)	0.4996(2)	0.08028(4)	0.02730(3)
Pb7	0.9348(2)	0.4892(2)	0.47581(4)	0.02730(3)
Pb8	0.2701(2)	−0.0361(2)	0.13120(4)	0.02730(3)
V1	0.3645(2)	1.0295(2)	0.24538(4)	0.04537(8)
V2	0.1825(1)	0.0020(1)	0.00651(4)	0.04537(8)
V3	0.0290(1)	−0.4555(1)	0.60116(3)	0.04537(8)
V4	0.3447(1)	0.4713(2)	0.86100(4)	0.04537(8)
O11	0.41282	1.24586	0.20892	0.04537(8)
O12	0.18774	1.10429	0.27414	0.04537(8)
O13	0.31937	0.78582	0.21423	0.04537(8)
O14	0.53804	0.98201	0.28424	0.04537(8)
O21	0.11697	−0.14213	0.05336	0.04537(8)
O22	0.08940	−0.11944	−0.04283	0.04537(8)
O23	0.11991	0.28199	0.00921	0.04537(8)
O24	0.40354	−0.01259	0.00628	0.04537(8)
O31	0.14165	−0.55079	0.65029	0.04537(8)
O32	−0.18289	−0.54138	0.60097	0.04537(8)
O33	0.03774	−0.16351	0.59929	0.04537(8)
O34	0.11949	−0.56619	0.55407	0.04537(8)
O41	0.32530	0.24206	0.89673	0.04537(8)
O42	0.39404	0.71022	0.89325	0.04537(8)
O43	0.50665	0.42023	0.82525	0.04537(8)
O44	0.15283	0.51281	0.82875	0.04537(8)
O1	0.3751(3)	0.2245(3)	0.72642(8)	0.02761(8)
O2	0.3377(3)	0.7216(3)	0.72151(7)	0.02761(8)
O3	0.3398(3)	0.2821(3)	0.38365(8)	0.02761(8)
O4	0.1890(2)	0.2215(3)	0.46499(7)	0.02761(8)
O5	0.0459(2)	0.7270(3)	0.14450(8)	0.02761(8)
O6	0.3753(3)	0.7525(3)	0.38814(7)	0.02761(8)
O7	0.0635(2)	0.2319(3)	0.14362(7)	0.02761(8)
O8	0.1950(2)	0.7241(3)	0.46655(6)	0.02761(8)

[a]CCDC reference numbers 181969 and 181970. See http://www.rsc.org/suppdata/jm/b2/b202648a/ for crystallographic files in CIF or other electronic format.

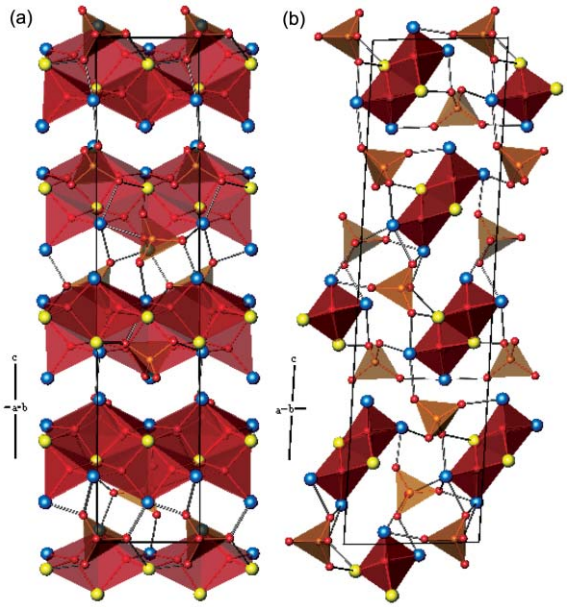

Fig. 2 Views of the α-$BiPb_2VO_6$ structure down (a) the *a* axis and (b) the *b* axis: Bi atoms are depicted in yellow, Pb atoms in blue, V atoms in light brown and O in red; light brown tetrahedra represent VO_4 groups; red tetrahedra represent OBi_2Pb_2 groups which share edges and form chains running along the *b* axis.

This then suggested a unit cell of $a = 6.03828(1)$ Å, $b = 9.44267(2)$ Å and $c = 12.07438(4)$ Å, which is related to the metrically tetragonal unit cell by the transformation matrix:

$$\begin{matrix} 0 & 1 & 1 \\ 0 & 1 & 0 \\ \frac{1}{2} & 0 & 0 \end{matrix}$$

An asymmetric unit in space group *Cmcm* containing one crystallographically unique Bi, Pb and V atom was then constructed. This model was used for Rietveld refinement of the high temperature X-ray diffraction data and gave an excellent fit. The same partial model containing metals only was then refined against the neutron data and a difference Fourier map revealed the positions of three oxygen atoms: one unique oxygen atom tetrahedrally coordinated by two Bi and two Pb atoms, and two other oxygen atoms forming a tetrahedral coordination environment around V. However, there were still significant discrepancies when this full structural model was used to perform a Rietveld refinement of the neutron data. A similar situation was previously encountered in $BiMg_2AO_6$ (A = V, P) phases.[7,8] The symmetry was therefore reduced to the primitive orthorhombic space group *Pmcn*, with one Bi, two Pb, one V and four crystallographically unique O atoms in the asymmetric unit. A model for simulated annealing was constructed with three unique oxygen atoms forming a rigid VO_4 group. Several thousand cycles of simulated annealing were then performed in which tetrahedral positions and rotations were moved to random values (subject to symmetry constraints), followed by Rietveld refinement against both X-ray and neutron data sets. After convergence random shifts were applied to the various degrees of freedom of the structural model, followed by re-refinement. This resulted in a model showing excellent agreement with both sets of data. In subsequent cycles of Rietveld refinement, the positional parameters and isotropic temperature factors of all atoms were refined against both data sets. The obtained agreement factors were: overall $wR_p = 9.984\%$, $wR_p = 11.148\%$ and $R_{Bragg} = 8.328\%$ for X-ray data and $wR_p = 7.342\%$ and $R_{Bragg} = 7.542\%$ for neutron data. A full anisotropic refinement was carried out against high resolution neutron diffraction data only and the agreement factors obtained were $wR_p = 5.513\%$ and $R_{Bragg} = 2.329\%$.

It became apparent from this refinement that the magnitude of the anisotropic displacement parameters was such that one might expect some artificial shortening of the V–O bonds due to correlated atomic motions (*cf.* the torsion/libration/screw (TLS) model for molecular systems[21]). In final cycles of refinement the mean V–O distance was therefore allowed to refine to 1.637(3) Å. This resulted in a small, but significant improvement in the fit, with agreement factors of $wR_p = 5.354\%$ and $R_{Bragg} = 1.570\%$.

The final Rietveld plots are given in Fig. 3, the atomic coordinates in Table 2 and the atomic displacement parameters in Table 3. Views of the structure of δ-$BiPb_2VO_6$ are shown in Fig. 4.

Comparison of α-$BiPb_2VO_6$ and δ-$BiPb_2VO_6$

The views of δ-$BiPb_2VO_6$ depicted in Fig. 4 show that the building blocks of the crystal structure, namely the OBi_2Pb_2 and VO_4 tetrahedra display a clear resemblance to the features of α-$BiPb_2VO_6$.

In the high temperature form, there is one unique oxygen atom coordinated tetrahedrally by heavy metals Bi and Pb, forming the OM_4 unit. In δ-$BiPb_2VO_6$ the range of the O–M–O angles is between 98° and 119°, while the scatter is wider at room temperature, reflecting a higher degree of distortion of these groups from the ideal tetrahedral geometry with the descent in symmetry. However, the edge-sharing pattern of OBi_2Pb_2 groups and the mutual orientation of the one-dimensional infinite chains they form, remain unchanged.

The principal difference between the structures of the two forms of $BiPb_2VO_6$ arises from the orientations of the isolated VO_4 tetrahedral groups. Both phases contain a motif formed by a total of six VO_4 groups surrounding a chain of

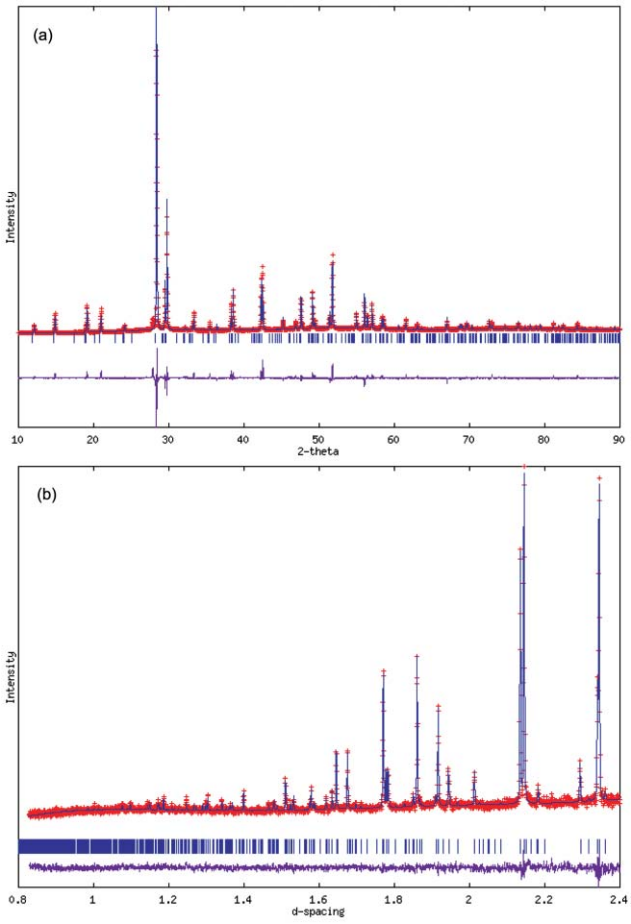

Fig. 3 Final Rietveld plots for (a) X-ray and (b) time-of-flight neutron data for δ-$BiPb_2VO_6$.

Table 2 Atomic coordinates for δ-$BiPb_2VO_6$ at 680 °C

Site	x	y	z	U_{iso}/Å^2
Bi1	0.75000	0.0051(6)	0.8974(2)	0.105(1)
Pb1	0.75000	−0.7100(6)	0.0965(4)	0.111(2)
Pb2	0.25000	−0.7116(6)	0.8981(4)	0.107(2)
V1	0.25000	0.029(1)	0.6894(6)	0.101(5)
O11	0.48242	0.13250	0.70571	0.41(1)
O12	0.25000	−0.10305	0.78707	0.44(2)
O13	0.25000	−0.04416	0.56912	0.26(1)
O1	0.024(2)	−0.8419(7)	0.989(1)	0.096(2)

Table 3 Atomic displacement parameters (Å^2) for δ-$BiPb_2VO_6$ at 680 °C (V fixed at combined refinement values)

Atom	U_{11}	U_{22}	U_{33}	U_{23}	U_{13}	U_{12}
Bi1	0.070(1)	0.155(1)	0.114(1)	−0.051(1)	0	0
Pb1	0.251(4)	0.155(3)	0.091(1)	−0.071(4)	0	0
Pb2	0.111(3)	0.089(2)	0.131(2)	0.026(3)	0	0
V1	0.101	0.101	0.101	0	0	0
O11	0.095(2)	0.38(1)	0.29(1)	0.184(7)	0.074(5)	0.10(1)
O12	0.97(6)	0.67(4)	0.24(1)	0.02(5)	0	0
O13	0.54(1)	0.44(1)	0.117(3)	−0.18(1)	0	0
O1	0.115(2)	0.109(1)	0.203(2)	0.018(1)	−0.020(1)	−0.032(2)

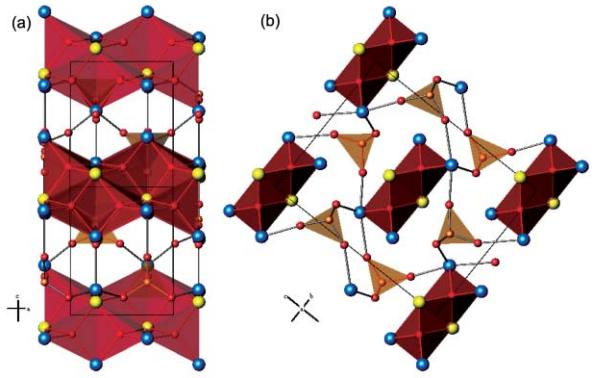

Fig. 4 Views of the δ-$BiPb_2VO_6$ structure down (a) the <110> direction and (b) the *a* axis: Bi atoms are depicted in yellow, Pb atoms in blue, V atoms in light brown and O in red; light brown tetrahedra represent VO_4 groups.

edge-sharing OBi_2Pb_2 groups (Figs. 2b and 4b). In α-$BiPb_2VO_6$ four of these groups are crystallographically unique VO_4 tetrahedra, in δ-$BiPb_2VO_6$ only one.

In order to compare the distribution of oxygen atoms around the vanadium centers in the two forms, the symmetry elements of space group *Pmcn* relating four VO_4 groups, were applied to the four unique VO_4 tetrahedra of the low temperature structure. The resulting picture of the static distribution of oxygen atoms in the low-symmetry structure corresponds closely to the situation portrayed by the large atomic displacement parameters in the high-symmetry phase (Fig. 5).

We conclude that the high-temperature structure of δ-$BiPb_2VO_6$ is characterized by the presence of dynamically disordered VO_4 tetrahedra. On cooling to room temperature these tetrahedra adopt distinct ordered orientations and a descent in symmetry to monoclinic results.

Relationship to other BiM_2AO_6 phases

Compounds of the BiM_2AO_6 family reported so far have been described as consisting of infinite $(BiO_2)^-$ chains, isolated AO_4 tetrahedra and interspersed M cations. They all crystallize in orthorhombic C-centered or primitive space groups, with the exception of monoclinic $BiCu_2VO_6$ (which, however, has a very pronounced underlying orthorhombic substructure).[6–14] The present analysis shows that all members of the BiM_2AO_6 family can be described as consisting of edge-sharing OBi_2M_2 tetrahedra and isolated AO_4 tetrahedra, as shown in Figs. 6–9.

This representation is useful as it allows the rationalization of the structural types found for the BiM_2AO_6 family in terms of the AO_4 tetrahedra tilts.

The highest symmetry structure in this series is base-centered centrosymmetric orthorhombic and it has been found for $BiCd_2PO_6$ and for the high temperature forms of $BiMg_2AO_6$ (A = V, As, P) and $BiZn_2PO_6$. The tetrahedral A cation is located at the intersection of two mirror planes (site symmetry *mm*2). The two edges of the AO_4 tetrahedra formed by pairs of

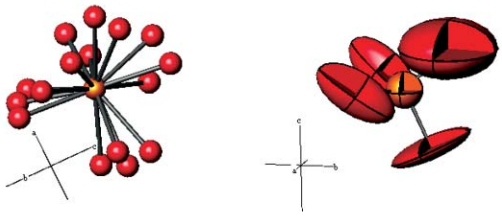

Fig. 5 Superposition of the unique VO_4 tetrahedra found in the room temperature structure of α-$BiPb_2VO_6$ compared with atomic displacement parameters (plotted at 50% probability) determined for the dynamically disordered δ-$BiPb_2VO_6$ form.

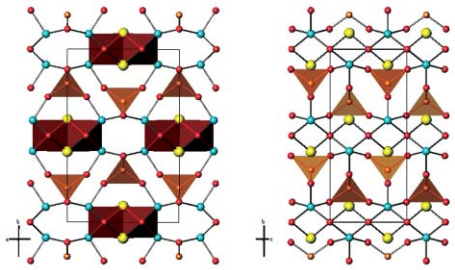

Fig. 6 Views of the high temperature $BiMg_2VO_6$ structure (space group *Amma*).

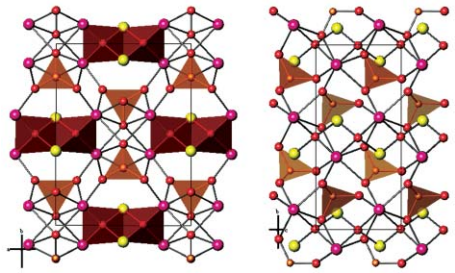

Fig. 7 Views of the $BiCa_2VO_6$ structure (space group $A2_1ma$).

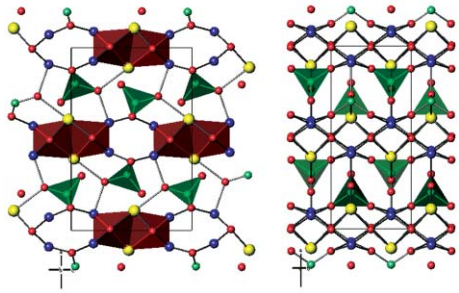

Fig. 8 Views of the $BiCu_2PO_6$ structure (space group *Pmcn*).

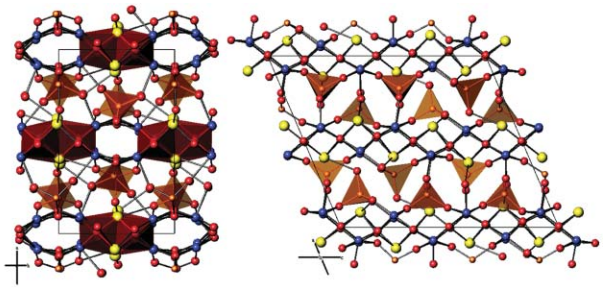

Fig. 9 Views of the $BiCu_2VO_6$ structure (space group $P2_1/n$).

symmetry related oxygen atoms are parallel to the normals to the mirror planes, which in the *Amma* setting correspond to crystallographic *a* and *b* axes (Figs. 6a and 6b). The lowering of symmetry in the other members of the BiM_2AO_6 family can be correlated to the AO_4 tetrahedral tilts relative to this high symmetry structure type.

Three phases, $BiCa_2VO_6$, $BiCa_2AsO_6$ and $BiCd_2VO_6$ crystallize in the noncentrosymmetric polar base-centered orthorhombic space group $A2_1ma$ (Fig. 7). The A cation lies on a mirror plane and a tetrahedral edge formed by two oxygen atoms related by this plane is parallel to the *b* axis (Fig. 7a). The remaining two unique oxygen atoms of the AO_4 groups are located on the same mirror plane and the tetrahedral edge they

Table 4 Deviations of primitive orthorhombic BiM_2AO_6 phases from the base-centered structure

Phase	Δ_y (fract)	b/Å	Δ_y/Å	$Tilt_b$/°
$BiMg_2PO_6$	0.001	7.8808(2)	0.0078	0.5
$BiMg_2VO_6$	0.008	7.9160(2)	0.0633	3.0
$BiZn_2PO_6$	0.019	7.8161(2)	0.1485	12.0
$BiCu_2PO_6$	0.034	7.7903(6)	0.2649	18.0
$BiPb_2PO_6$	0.063	9.08(1)	0.5720	Static disorder

form is tilted, so that all AO_4 tetrahedra point in the same direction along the crystallographic a axis (Fig. 7b). A comparison of Figs. 6b and 7b shows that this arrangement gives rise to a sevenfold coordination around the M^{2+} metal, which is a much more favorable environment for large species such as Ca and Cd ($^{VII}Ca^{2+}$ = 1.06 Å, $^{VII}Cd^{2+}$ = 1.03 Å)[22] than the fivefold coordination resulting from the centrosymmetric orientation of the AO_4 tetrahedra in $BiMg_2VO_6$.

Several phases, namely low temperature $BiMg_2AO_6$ (A = V, As, P) and $BiZn_2PO_6$, as well as $BiCu_2PO_6$, $BiCu_2AsO_6$, $BiPb_2PO_6$ and high temperature $BiPb_2VO_6$ adopt a primitive orthorhombic crystal structure in space group *Pmcn*. The A cations and two unique oxygen atoms of the AO_4 groups in these phases are located on a mirror plane and the only rotational degree of freedom for these tetrahedra is that about the crystallographic a axis (Fig. 8a). In these phases, the degree of symmetry lowering can be expressed in terms of the deviations of atomic positions from the base-centered case and the resulting tilts of the AO_4 tetrahedra. For the A cations, this is represented by the difference between the actual coordinates (¼, y, z) and those corresponding to the base-centered case (¼, 0, z). This value correlates very well with the magnitude of the tilts of the AO_4 tetrahedra relative to the b axis, as shown in Table 4.

$BiCu_2VO_6$ crystallizes in the monoclinic space group $P2_1/n$, with a unit cell volume three times that of the orthorhombic phases of the BiM_2AO_6 family (Fig. 9). There are three unique VO_4 tetrahedra in the structure, characterized by different tilt angles with respect to the crystallographic axes. They result in a fivefold coordination for two thirds and a sixfold coordination for the remaining third of the Cu atoms.

Hence all the known phases in this family are mutually related and the structural differences between the individual members can be related to the bonding preferences of the constituent species. Specifically in the case of $BiPb_2VO_6$, the significant lowering of the symmetry can be attributed to the presence of two lone pair cations (Bi^{3+} and Pb^{2+}) in this compound. This feature is encountered in other known families.[23]

The proposed view of the BiM_2AO_6 family structures as consisting of edge-sharing OBi_2M_2 tetrahedra and isolated AO_4 tetrahedra not only allows a systematic description of these compounds, but also facilitates the understanding of their phase transitions as a function of temperature, as illustrated by the title compound.

Acknowledgements

We would like to acknowledge the provision of neutron beam time by the CCLRC and EPSRC at the ISIS facility at the Rutherford Appleton Laboratories, UK and thank Kevin S. Knight for the assistance with the data collection. The high temperature X-ray facilities have been provided by the EPSRC/JREI grant number GR/M35222. JAKH thanks the EPSRC for a Senior Research Fellowship.

References

1 E. C. Subbarao, *J. Chem. Phys.*, 1961, **34**(2), 695.
2 P. Shuk, H. D. Wiemhoefer, U. Guth, W. Goepel and M. Greenblatt, *Solid State Ionics*, 1996, **89**, 179.
3 A. W. Sleight, *Science*, 1980, **208**, 895.
4 P. S. Halasyamani and K. R. Poeppelmeier, *Chem. Mater.*, 1998, **10**(10), 2753.
5 J. C. Boivin and G. Mairesse, *Chem. Mater.*, 1998, **10**(10), 2780.
6 I. Radosavljevic, J. S. O. Evans and A. W. Sleight, *J. Solid State Chem.*, 1998, **137**, 143.
7 I. Radosavljevic, J. A. K. Howard and A. W. Sleight, *Int. J. Inorg. Mater.*, 2000, **2**, 543.
8 I. Radosavljevic and A. W. Sleight, *J. Solid State Chem.*, 2000, **149**, 143.
9 F. Abraham, M. Ketatni, G. Mairesse and B. Mernari, *Eur. J. Solid State Inorg. Chem.*, 1994, **31**, 313.
10 I. Radosavljevic, J. S. O. Evans and A. W. Sleight, *J. Solid State Chem.*, 1998, **141**, 149.
11 I. Radosavljevic, J. S. O. Evans and A. W. Sleight, *J. Alloys Compd.*, 1999, **284**, 99.
12 E. M. Ketatni, B. Memari, F. Abraham and O. Mentre, *J. Solid State Chem.*, 2000, **153**, 48.
13 A. Mizrahi, J. P. Wignacourt and H. Steinfink, *J. Solid State Chem.*, 1997, **133**, 516.
14 A. Mizrahi, J. P. Wignacourt, M. Drache and P. Conflant, *J. Mater. Chem.*, 1995, **5**(6), 901.
15 S. Giraud, A. Mizrahi, M. Drache, P. Conflant, J. P. Wignacourt and H. Steinfink, *Solid State Sci.*, 2001, **3**, 593.
16 X. Xun, S. Uma and A. W. Sleight, in press.
17 I. Radosavljevic Evans, J. A. K. Howard, R. L. Withers and J. S. O. Evans, *Chem. Commun.*, 2001, 1984.
18 A. Altomare, M. C. Burla, G. Cascarno, C. Giacovazzo, A. Guagliardi, A. G. G. Moliterni and G. Polidori, *J. Appl. Crystallogr.*, 1995, **28**, 842.
19 Topas v2.0: General Profile and Structure Analysis Software for Powder Diffraction Data, Bruker AXS, Karlsruhe, Germany, 2000.
20 G. S. Pawley, *J. Appl. Crystallogr.*, 1981, **14**, 357.
21 V. Schomaker and K. N. Trueblood, *Acta Crystallogr., Sect. B*, 1968, **24**, 63.
22 R. D. Shannon, *Acta Crystallogr., Sect. A*, 1976, **32**, 751.
23 R. D. Shannon, J. D. Bierlein, J. L. Gillon, G. A. Jones and A. W. Sleight, *J. Phys. Chem. Solids*, 1980, **41**, 117.